Supporting Information

Doxorubicin-Based Ionic Nanomedicines for Combined Chemo-Phototherapy of Cancer

Mujeebat Bashiru,[1] Samantha Macchi,[1] Mavis Forson,[1] Amna Khan,[2] Arisha Ishtiaq,[1] Adeniyi Oyebade,[1] Amanda Jalihal,[1] Nawab Ali,[3] Robert J. Griffin,[4] Adegboyega K Oyelere,[5] Nasrin Hooshmand,[6] Noureen Siraj* [1]

[1]*Department of Chemistry, University of Arkansas at Little Rock, Little Rock, AR 72204, USA.*

[2]*Department of Chemistry, University of Arkansas at Fayetteville, AR 72701, USA.*

[3]*Department of Biology, University of Arkansas at Little Rock, Little Rock, AR 72204, USA.*

[4]*University of Arkansas for Medical Sciences, Winthrop P. Rockefeller Cancer Institute, Arkansas Nanomedicine Center, Department of Radiation Oncology, 4301 W Markham St, Little Rock, AR 72205, USA.*

[5]*School of Chemistry and Biochemistry, Parker H. Petit Institute for Bioengineering and Bioscience, Georgia Institute of Technology, Atlanta, Georgia 30332, USA.*

[6]*Laser Dynamics Laboratory, School of Chemistry and Biochemistry, Georgia Institute of Technology, Atlanta, Georgia 30332, USA.*

Corresponding author: nxsiraj@ualr.edu

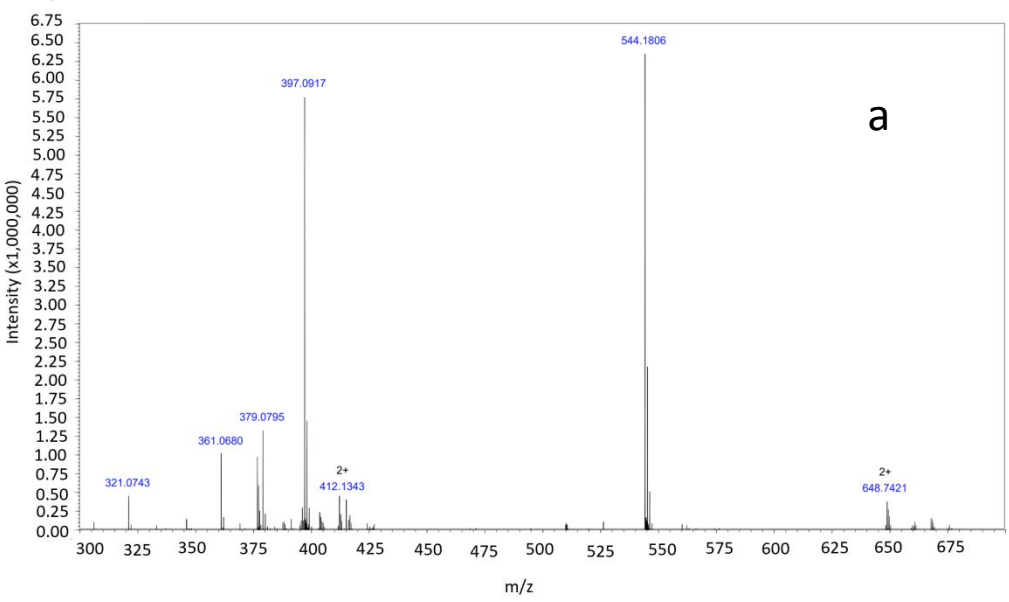

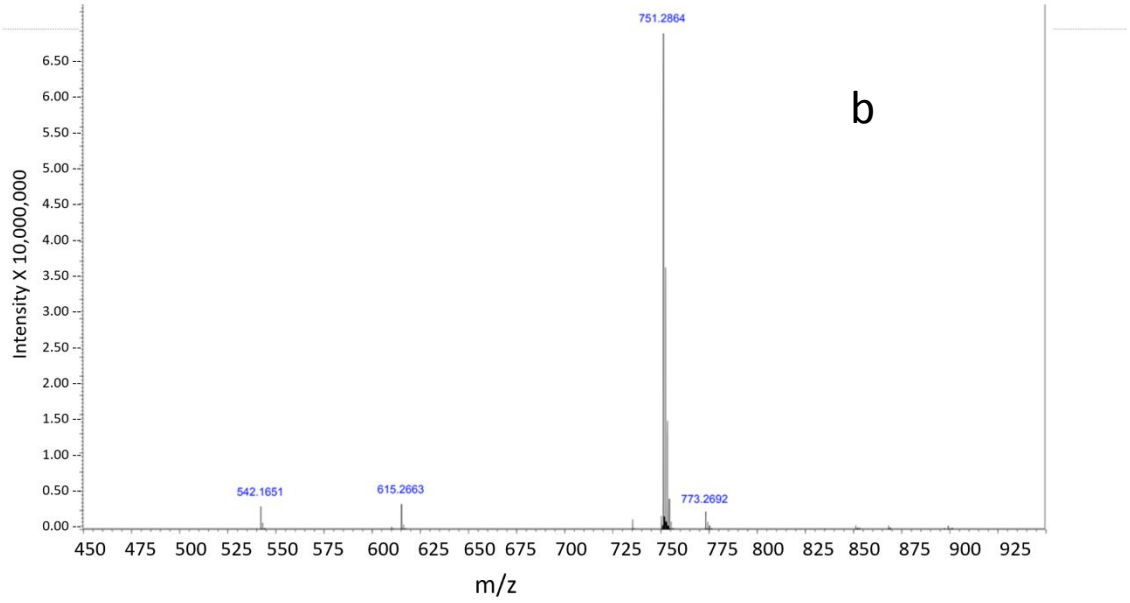
751.2864
b
Intensity X 10,000,000
6.50
6.00
5.50
5.00
4.50
4.00
3.50
3.00
2.50
2.00
1.50
1.00
0.50
0.00
542.1651
615.2663
773.2692
450 475 500 525 550 575 600 625 650 675 700 725 750 775 800 825 850 875 900 925
m/z

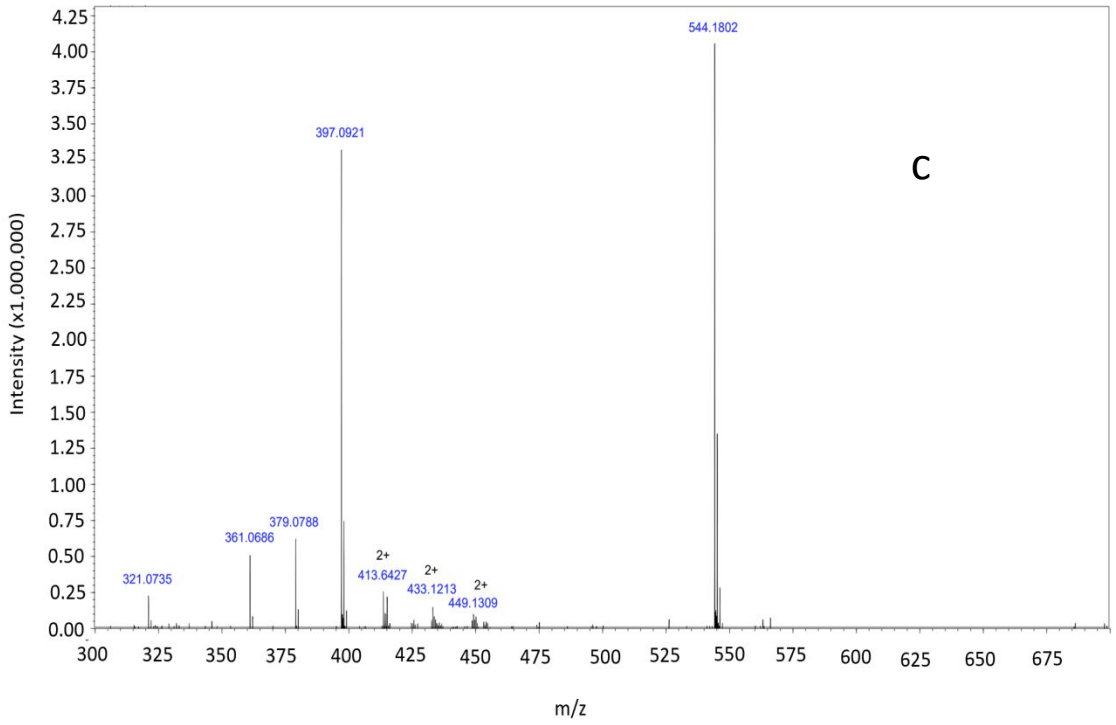
544.1802
397.0921
c
Intensity (x1,000,000)
4.25
4.00
3.75
3.50
3.25
3.00
2.75
2.50
2.25
2.00
1.75
1.50
1.25
1.00
0.75
0.50
0.25
0.00
379.0788
361.0686
321.0735
2+
413.6427
2+
433.1213
2+
449.1309
300 325 350 375 400 425 450 475 500 525 550 575 600 625 650 675
m/z

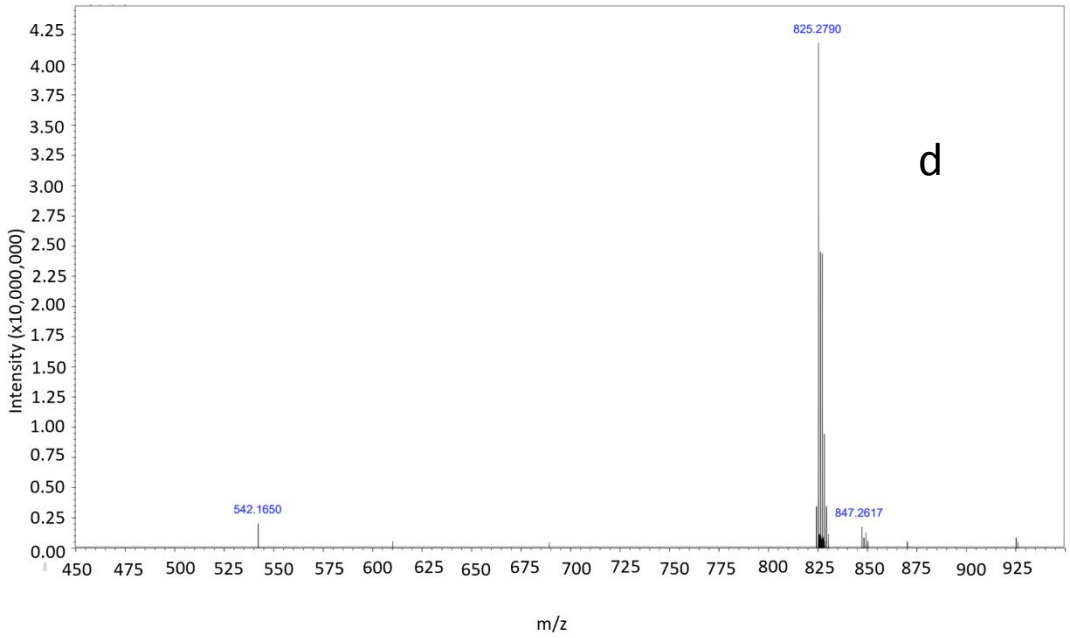
825.2790
542.1650
847.2617
Intensity (x10,000,000)
m/z
d

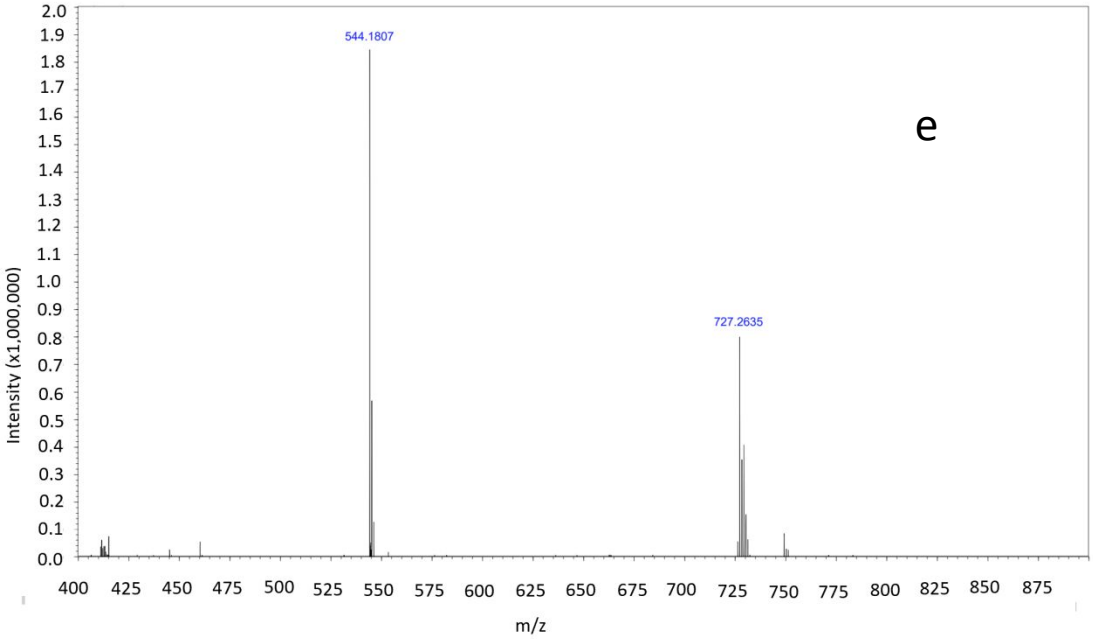
544.1807
727.2635
Intensity (x1,000,000)
m/z
e

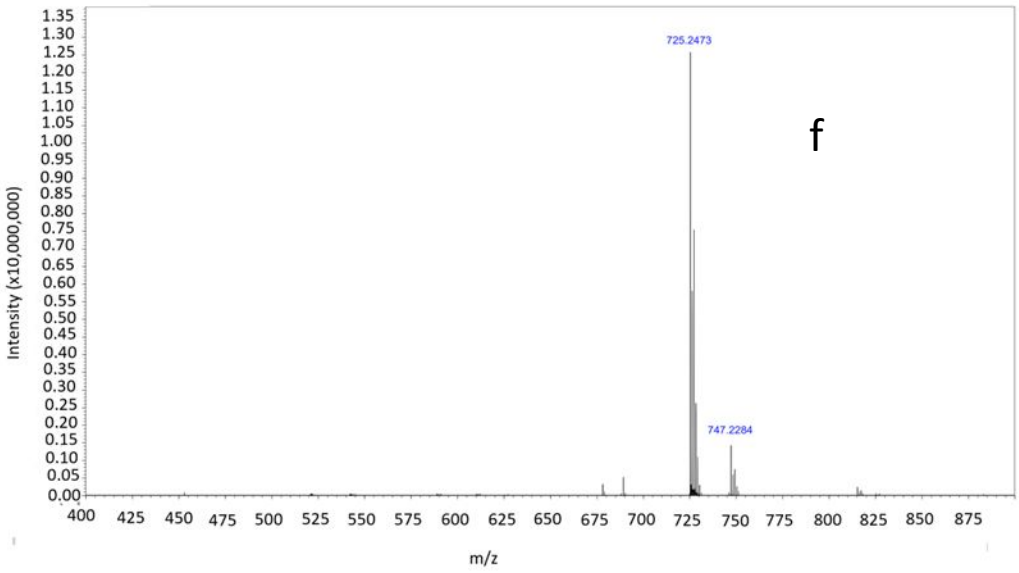

Figure S1. ESI-MS of a) [DOX][ICG] in positive ion mode b) [DOX][ICG] in negative ion mode c) [DOX][IR820] in positive ion mode d) [DOX][IR820] in negative ion mode e) [DOX][IR783] in positive ion mode f) [DOX][IR783] in negative ion mode.

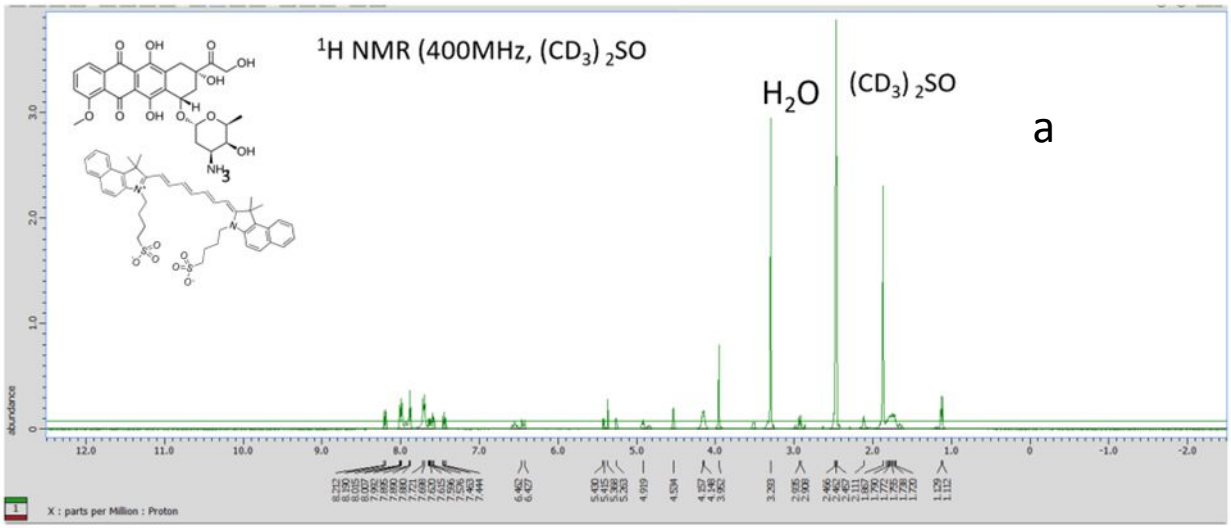

[DOX][ICG]-1 H NMR (400 MHz, DMSO-d_6): δ 1.2 (d, 3H), 1.9 (m, 22H), 2.1 (m, 2H), 3.0 (m, 2H), 3.6 (d, 1H), 4.0 (s, 3H), 4.2 (t, 5H), 4.6 (s, 2H), 5.0 (m, 2H), 5.3 (d, 1H), 5.4 (m, 2H), 6.5 (m, 4H), 7.5 (t, 2H), 7.6 (m, 9H), 8.0 (m, 8H), 8.2 (d, 2H).

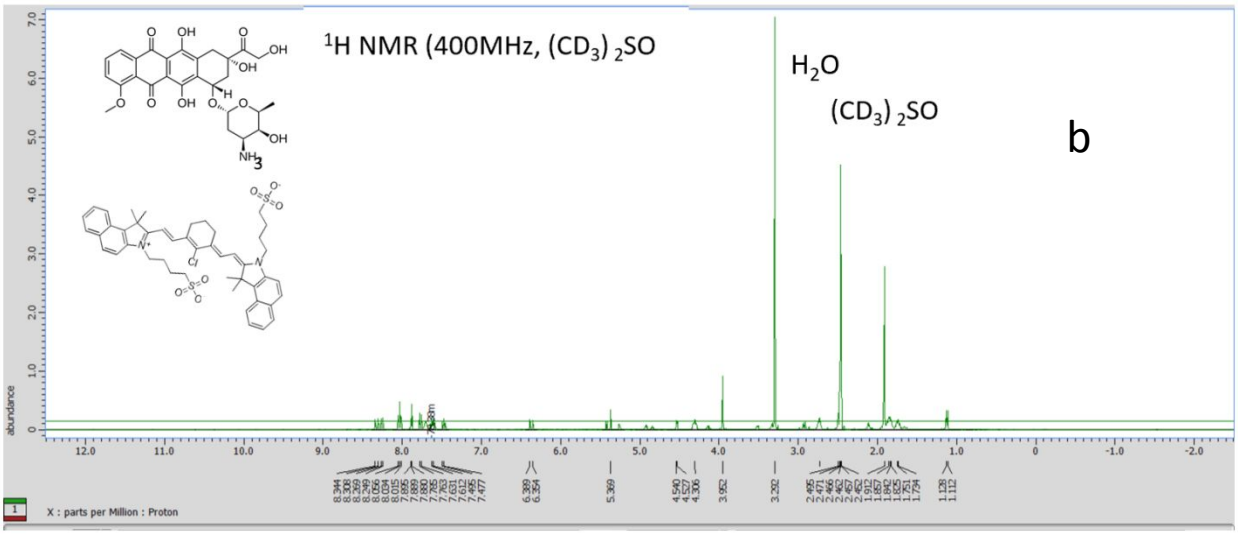

[DOX][IR820]- 1 H NMR (400 MHz, DMSO-d_6): δ 1.2 (d, 3H), 1.9 (m, 25H), 2.2 (d, 2H), 2.8 (d, 4H), 3.0 (m, 2H), 3.6 (d, 1H), 4.0 (s, 3H), 4.2 (t, 1H), 4.3 (t, 4H), 4.6 (d, 2H), 5.0 (m, 2H), 5.4 (m, 3H), 6.4 (d, 2H), 7.6 (m, 3H), 7.8 (m, 4H), 7.9 (m, 4H), 8.1 (t, 4H), 8.3 (m, 4H).

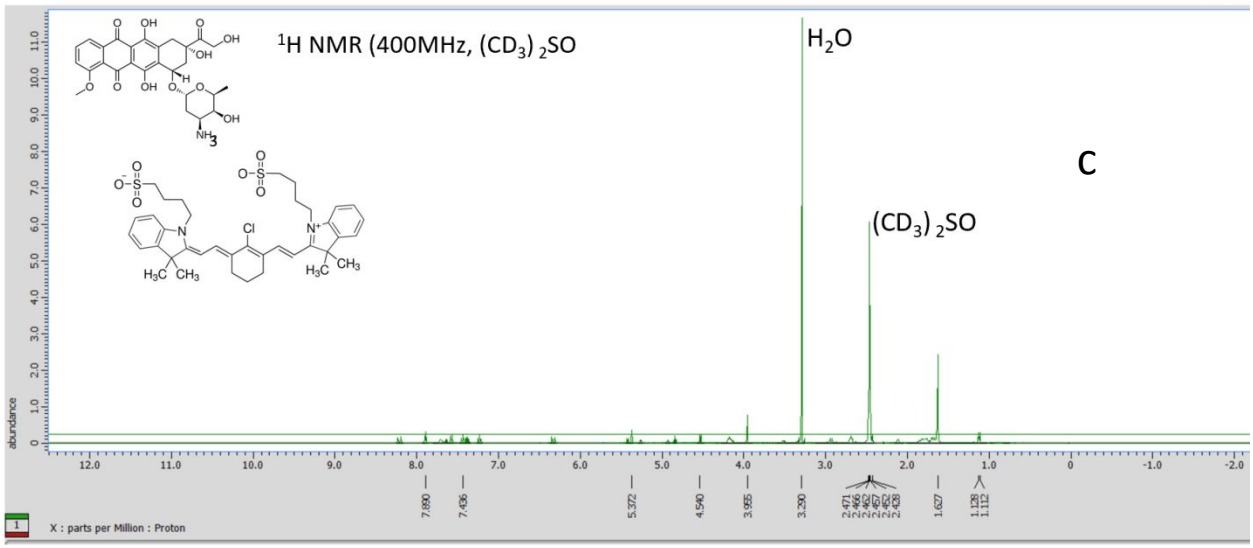

[DOX][IR783]-1 H NMR (400 MHz, DMSO-d_6): δ 1.2 (d, 3H), 1.7 (m, 10H), 1.9 (m, 3H), 2.1 (m, 1H), 2.7 (m, 4H), 3.0 (t, 2H), 3.6 (d, 1H), 4.0 (s, 3H), 4.2 (m, 5H), 4.6 (d, 2H), 4.9 (m, 2H), 5.4 (m, 3H), 6.4 (d, 2H), 7.3 (t, 2H), 7.5 (m, 4H), 7.7 (m, 5H), 7.9 (t, 2H), 8.3 (t, 2H).

Figure S2. NMR spectrum of a) [DOX][ICG], b)[DOX][IR820] and c) [DOX][IR783].

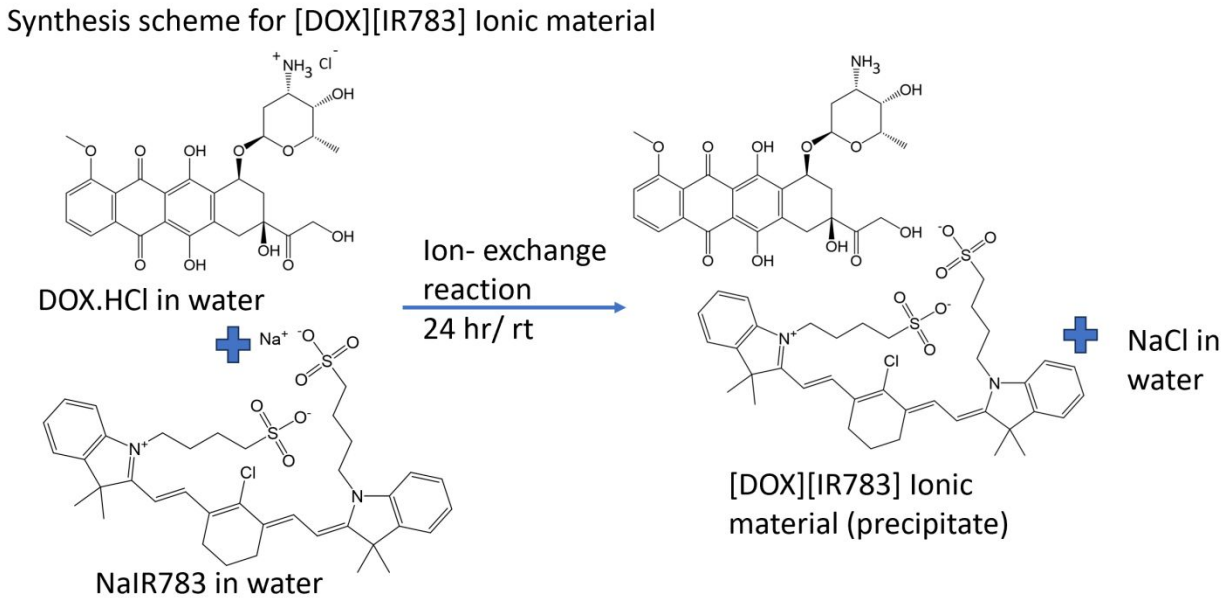

Figure S3. Synthesis of [DOX][IR783] ionic material using ion-exchange reaction.

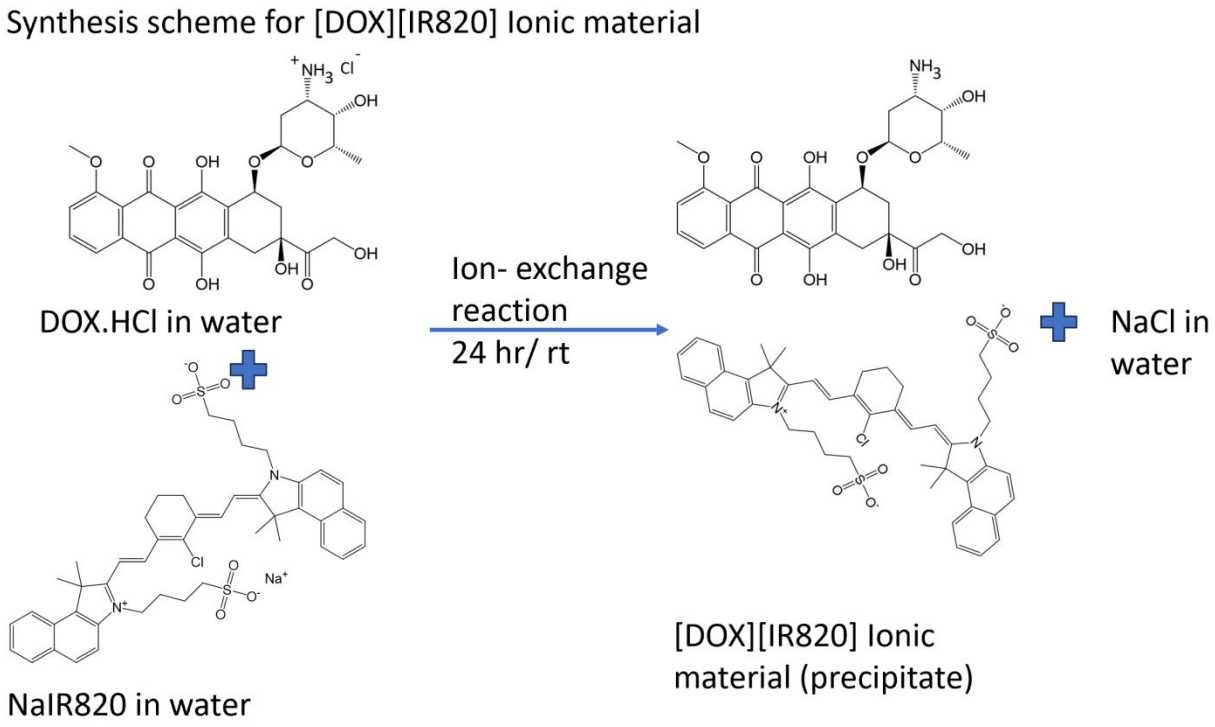

Figure S4. Synthesis of [DOX][IR820] ionic material using ion- exchange reaction.

Table S1. Melting point values of the synthesized IMs as compared to the free NIR dyes.

Drugs	**Melting point (°C)**
DOX	205-216
NaIR820	>300
NaIR783	209-212
NaICG	205-208
[DOX][ICG]	229-232
[DOX][IR820]	232-234
[DOX][IR783]	211-213

Table S2. Zeta potential and Polydispersity index for all INMs

INMs	Zeta potential (mV)	Polydispersity index
[DOX][ICG]	-27.65 ± 6.5	0.20
[DOX][IR820]	-28.17 ± 4.5	0.23
[DOX][IR783]	-12.75 ± 9.4	0.30

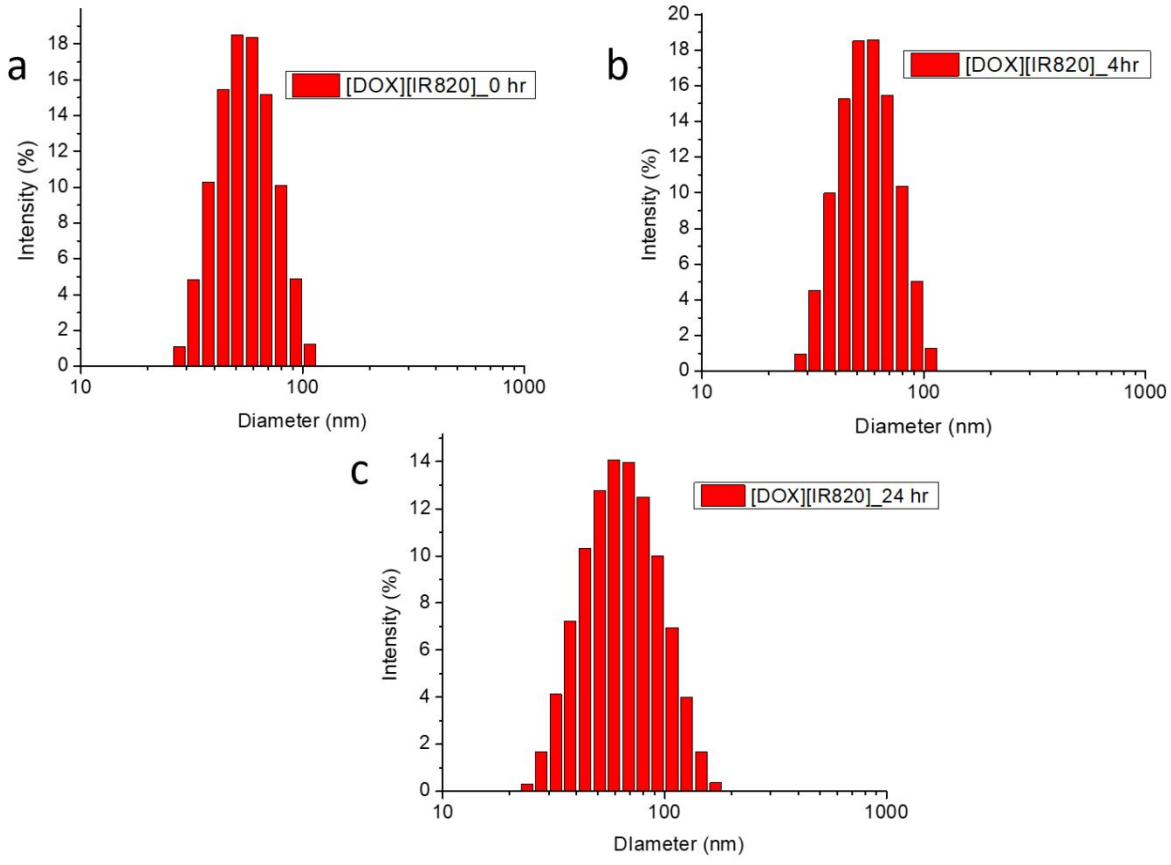

Figure S5. Time-dependent DLS plots for [DOX][IR820] INMs at a) 0th hr b) 4 hr c) 24 hr.

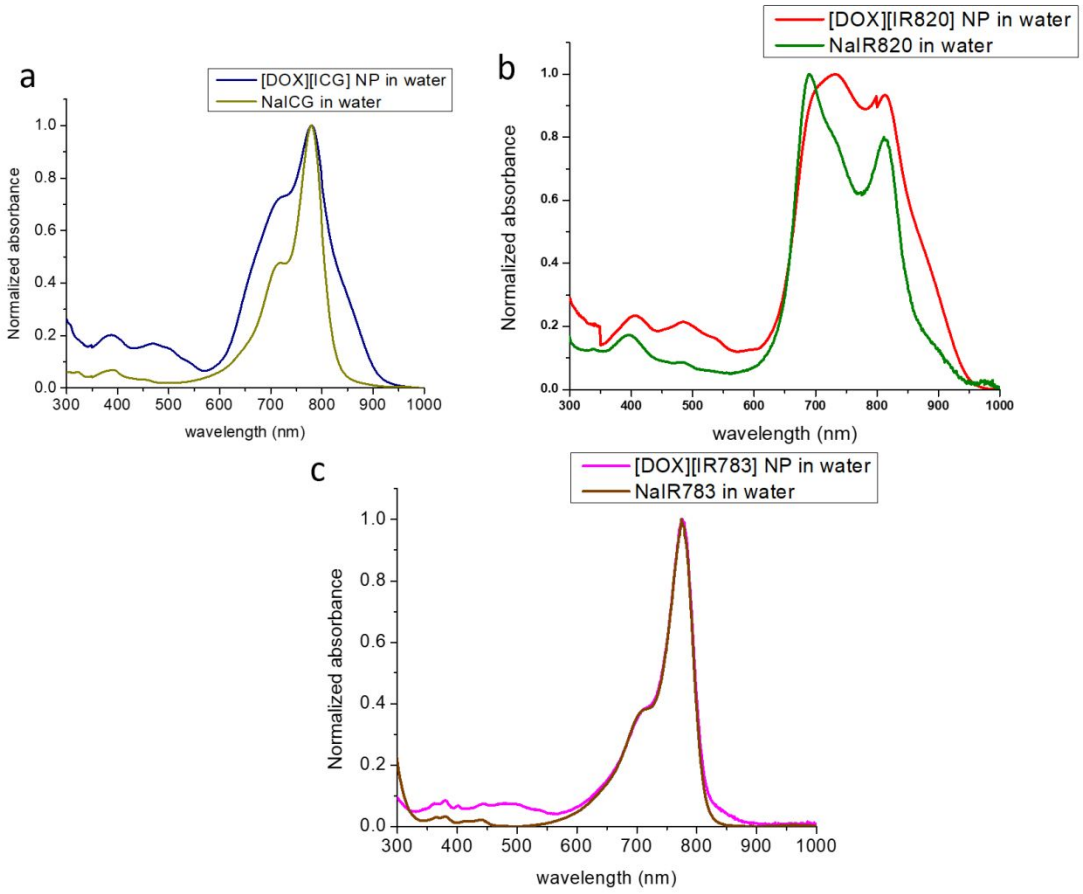

Figure S6. Normalized absorbance of a) [DOX][ICG] INMs and NaICG in water b) [DOX][IR820] INMs and NaIR820 in water c) [DOX][IR783] INMs and NaIR783 in water.

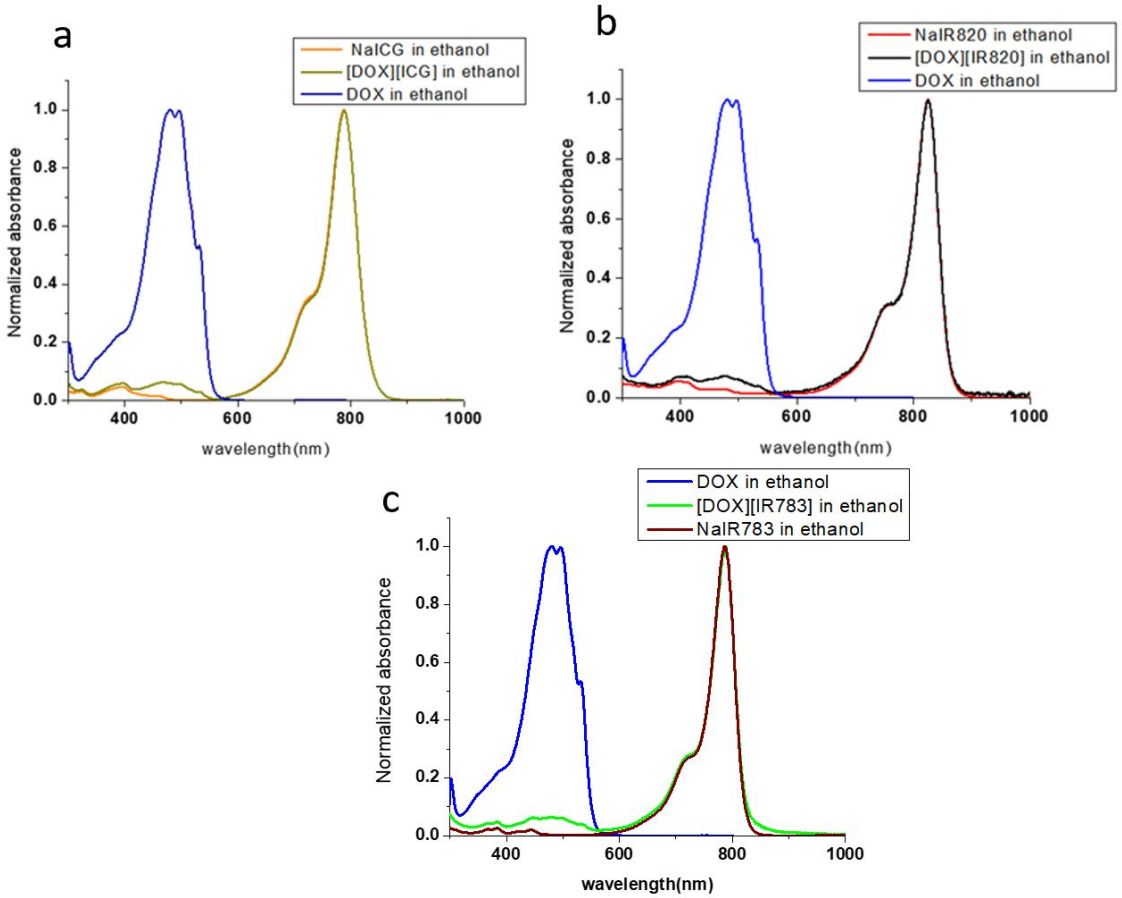

Figure S7. Normalized absorption spectra in ethanol for a) DOX, NaICG and [DOX][ICG] b) DOX, NaIR820 and [DOX][IR820] and c) DOX, NaIR783 and [DOX][IR783]

Table S3. Molar absorptivity values for parent dye, INMs and IMs in water and ethanol respectively

Compound (solvent)	λ_{max} (water/ethanol)	Molar extinction coefficient ($cm^{-1}M^{-1}$)
Doxorubicin in water/ethanol	480/480	9075/ 9225
NaIR820 in water/ ethanol	813/ 830	24642/ 272621
[DOX][IR820] in water (INM)/ ethanol (IMs)	813/ 830	39267/68941
NaIR783 in water/ ethanol	774/ 787	189883/ 386293
[DOX][IR783] in water (INM)/ ethanol (IM)	774/787	193927/ 260145
NaICG in water/ ethanol	777/ 789	247303/ 115600
[DOX][ICG] in water (INM)/ ethanol (IM)	777/789	138257/ 188000

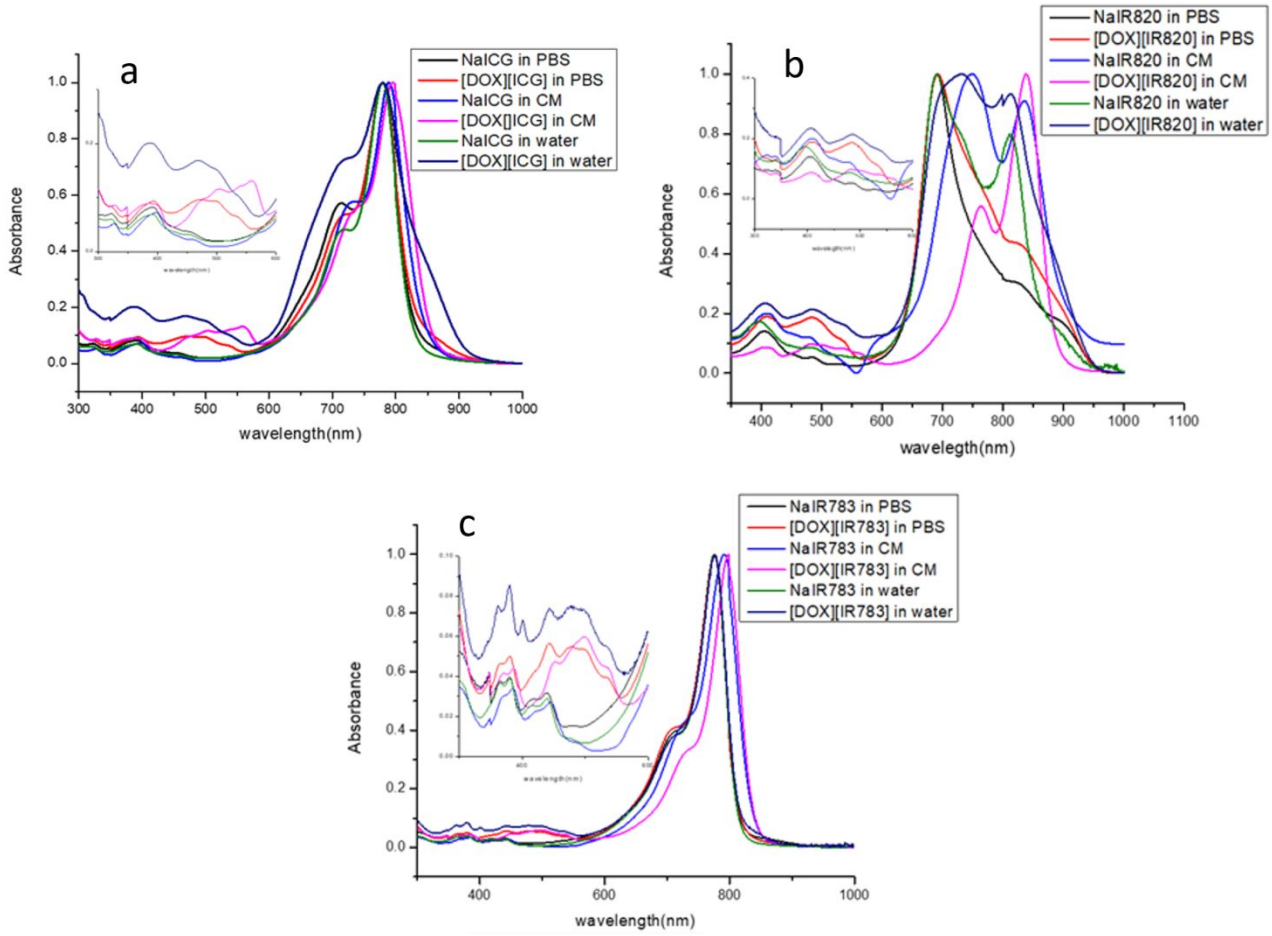

Figure S8. Absorption spectra in phosphate buffer saline (PBS), cell media (CM) and water for a) NaICG and [DOX][ICG] b) NaIR820 and [DOX][IR820] and c) NaIR783 and [DOX][IR783]

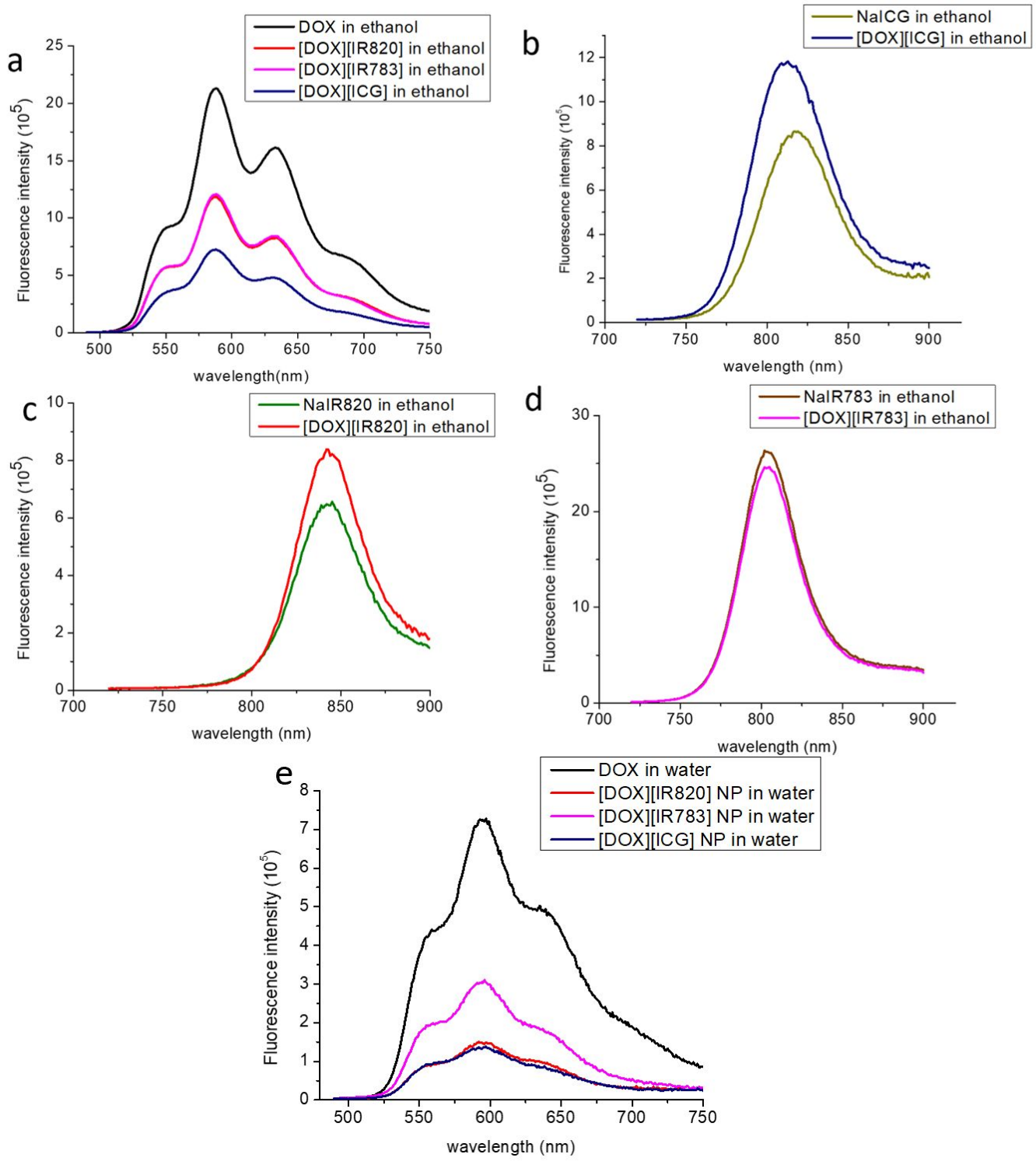

Figure S9. Fluorescence emission spectra of a) chemo-PTT combination IMs in ethanol at an exictation wavelngth of 480 nm, while all fluorescence spectra in b, c and d are recorded in ethanol at an excitation wavelngth of 710nm b) NaICG and [DOX][ICG] IMs c) NaIR820 and [DOX][IR820] IMs d) NaIR783 and

[DOX][IR783] IMs e) Fluorescence spectra of DOX and chemo-PTT combination INMs in water (nanoparticles) at an excitation wavelength of 480 nm.

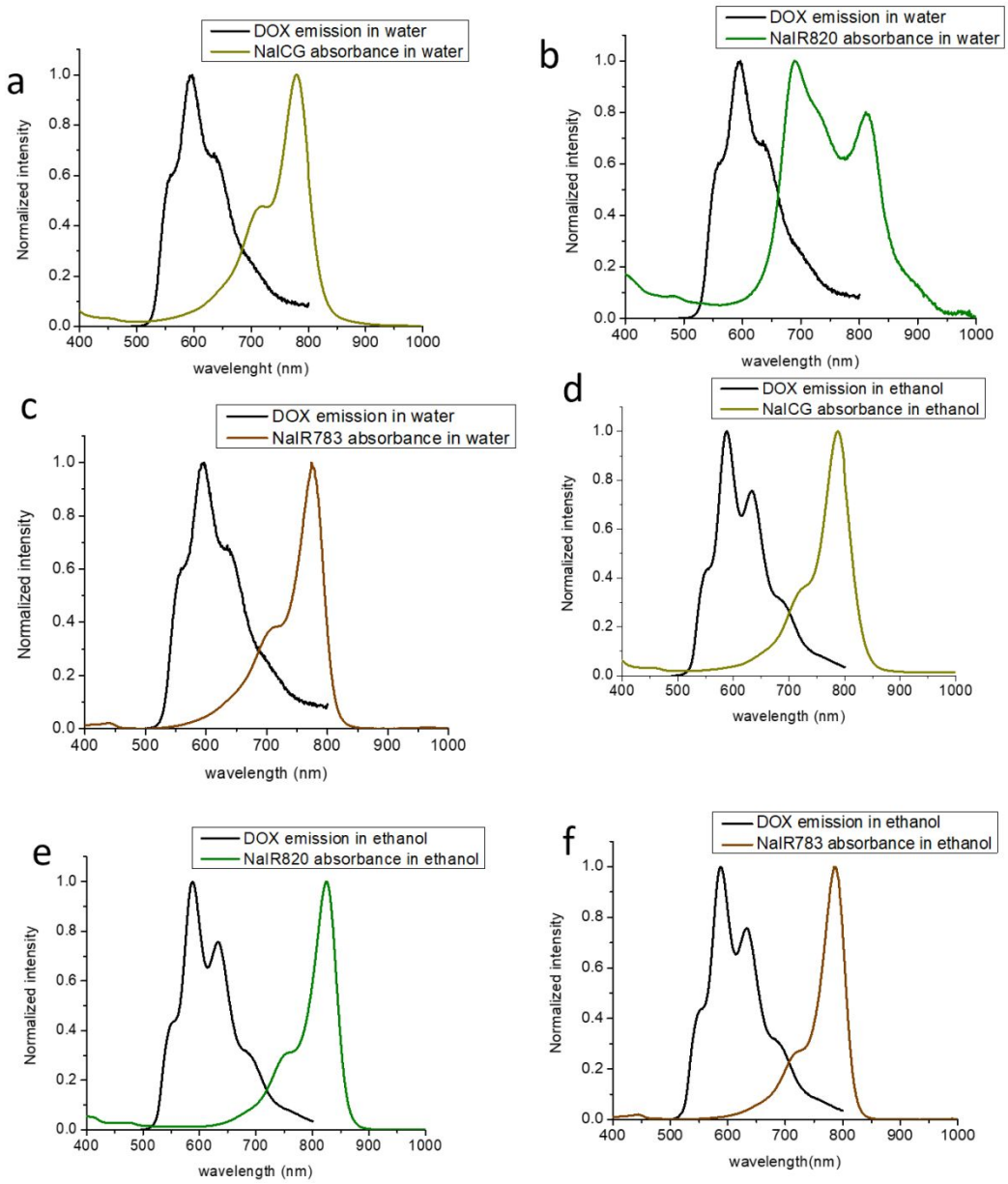

Figure S10. Normalized fluorescence emission spectra of a) DOX and NaICG absorption spectra in water b) DOX and NaIR820 absorption spectra in water c) DOX and NaIR783 absorption spectra in water d) DOX and NaICG absorption spectra in ethanol e) DOX and NaIR820 absorption spectra in ethanol f) DOX and NaIR783 absorption spectra in ethanol.

FRET Efficiency Equation

$$E = 1 - \frac{F_{da}}{F_d} \quad \text{-------(S1)}$$

where Fda is integrated fluorescence emission of the donor (DOX) in the presence of the acceptor (PTT dye) and Fd is the integrated fluorescence emission of the donor (DOX) in the absence of the acceptor.

$$J(\lambda) = \frac{\int_0^\infty \varepsilon(\lambda) f(\lambda) \lambda^4 d\lambda}{\int_0^\infty f(\lambda) d\lambda} \quad \text{-------(S2)}$$

Equation S2 quantifies the spectral overlap integral (J(λ)) where ε(λ) is the molar extinction coefficient ($M^{-1}cm^{-1}$) of acceptor (NIR dye) at overlap wavelength λ, and f(λ) is the normalized fluorescence intensity of DOX at overlap wavelength with NIR dye when excited at 480 nm.

$$R_0 = 0.0211(n^{-4} \times k^2 \times \Phi_d \times J)^{\frac{1}{6}} \quad \text{----------(S3)}$$

R_0 represents the Forster distance in IM or INM, where Φ_d is quantum yield of the donor (DOX) in the absence of the acceptor. *n* is refractive index of the media; *J* is the spectral overlap integral between donor and acceptor and k^2 is the dipole orientation factor.

Table S4. FRET efficiency for all INMs in the presence of DOX (donor).

INM	% FRET efficiency	Forster distance, R_o (nm)	Spectra overlap $X10^{16}$
[DOX][ICG]	81.0	3.49	1.59
[DOX][IR820]	79.8	3.44	1.47
[DOX][IR783]	60.5	3.47	1.53

Table S5. FRET efficiency for all IMs in the presence of DOX (donor).

IM	% FRET efficiency	Forster distance, Ro (nm)	Spectra overlap $X10^{16}$
[DOX][ICG]	67.6	8.41	1.72
[DOX][IR820]	46.4	8.85	2.33
[DOX][IR783]	45.9	8.52	1.85

Fluorescence quantum yield and photophysical rate constants

Fluorescence quantum yield of the donor (DOX) was determined using the relative method as shown in Equation S4. The quantum yield is determined with relative to a standard sodium fluorescein (NaFl), with a literature reported quantum yield value of 0.92 in water. [1]

$$\Phi_{un} = \Phi_{std} * \frac{I_{un}}{I_{std}} * \frac{Abs_{std}}{Abs_{un}} * (\frac{n_{un}}{n_{std}})^2 \text{--------(S4)}$$

where Φ_{std} is the quantum yield of the standard, I is the integrated emission intensity. Abs is the absorbance at the excitation wavelength (480 nm), and *n* is the refractive index of the standard (std) and unknown.

Fluorescence quantum yield of IMs and INMs were also determined for NIR compounds using the relative method. The quantum yield was determined using a relative method where NaIR820 was used as a standard as shown in Equation S4.

where Φ_{std} is the quantum yield of the standard, I is the integrated emission intensity. Abs is the absorbance at the excitation wavelength, and *n* is the refractive index of the standard (std) and unknown(un). ICG was used as a standard with a reported FLQY value of 0.14[2] in ethanol.

From the absorption and fluorescence emission spectra, the radiative rate constant (k_{rad}) was also calculated using the Stricker-Berg relationship (Equation S6)

$$k_{rad} = 2.88 * 10^{-9} * \frac{\int(\bar{\nu})d\bar{\nu}}{\int I(\bar{\nu})\bar{\nu}^{-3}} * \int\frac{\varepsilon(\bar{\nu})}{\bar{\nu}}d\bar{\nu} \text{---------(S5)}$$

where I represent the emission intensity, $\bar{\nu}$ is the wavenumber of light, and Ɛ is the molar extinction coefficient.

Using the radiative rate constant, the non-radiative rate constant ($k_{non-rad}$) was calculate for each compound using Equation S6

$$\Phi_F = \frac{k_{rad}}{k_{rad} + k_{non-rad}} \text{ ----------(S6)}$$

Table S6: Fluorescence quantum yield ($\boldsymbol{\phi}_F$), radiative rate (k_{rad}), and non-radiative rate ($k_{non\text{-}rad}$) of all IMs in ethanol at an excitation wavelength of 710 nm.

Drugs (IMs)	$\boldsymbol{\phi}_F$ (%)	K_{rad} ($10^7 s^{-1}$)	$K_{non\text{-}rad}$ ($10^7 s^{-1}$)
NaICG	14.0	4.3	26.5
[DOX][ICG]	19.4	4.4	18.2
NaIR820	9.6	4.6	42.8
[DOX][IR820]	11.4	5.0	38.8
NaIR783	31.0	5.1	11.3
[DOX][IR783]	30.1	4.8	11.1

Table S7. Fluorescence quantum yield ($\boldsymbol{\phi}_F$) of INMs and IMs in water and ethanol at an excitation wavelength of 480 nm. DOX was used as reference with a reported literature fluorescence quantum yield of 9 %[3]

Drugs	$\boldsymbol{\phi}_F$ INMs (%)	$\boldsymbol{\phi}_F$ IMs (%)
DOX	9.0	9.0
[DOX][ICG]	2.0	10.0
[DOX][IR820]	7.0	6.0
[DOX][IR783]	1.0	18.0

Table S8. Fluorescence lifetimes of 10 μM combination drugs in ethanol recorded at 455 nm excitation/590 nm emission.

Sample	τ_1 (ns)	α_1	τ_2 (ns)	α_2	τ_3 (ns)	α_3	τ_{avg} (ns)	$\chi 2$
DOX	1.27	82.03	2.12	17.97	N/A	N/A	2.33	1.16
[DOX][ICG]	0.47	10.15	1.46	81.82	4.15	8.03	2.02	1.00
[DOX][IR820]	1.35	87.96	3.26	12.04	N/A	N/A	2.30	1.07
[DOX][IR783]	1.32	74.52	1.90	9.84	4.42	1.05	2.54	1.07

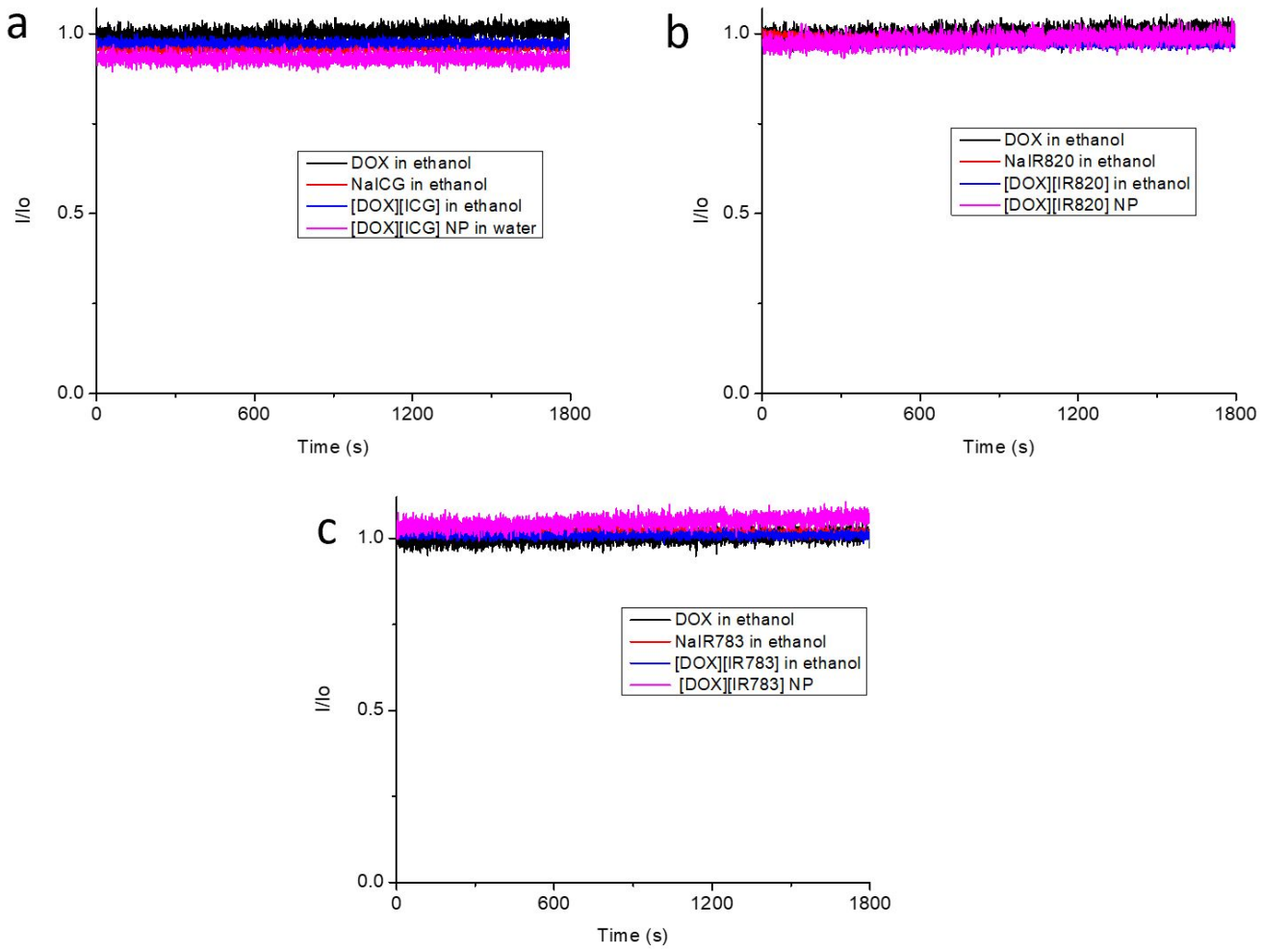

Figure S11. Photostability results for a) [DOX][ICG] INM and IM in water and ethanol.

b) [DOX][IR820] INM and IM in water and ethanol c) [DOX][IR783] INM and IM in water and ethanol

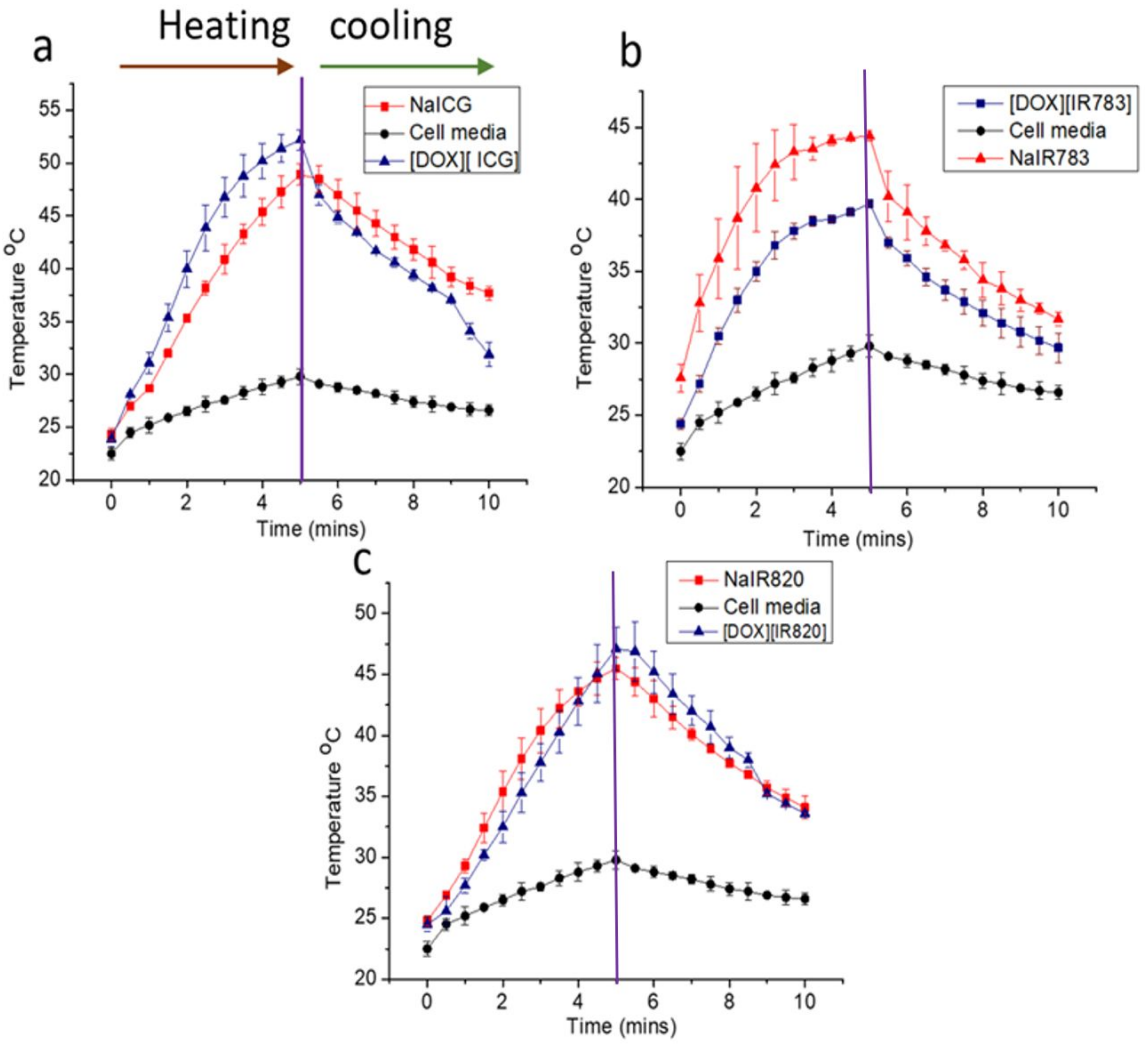

Figure S12. Light to heat conversion efficiency curve for a) [DOX][ICG] INMs and NaICG b) [DOX][IR783] INMs sand NaIR783 c) [DOX][IR820] INMs and NaIR820 in cell media conducted for 5-10 mins. Error bars are presented as mean ± standard deviation (SD).

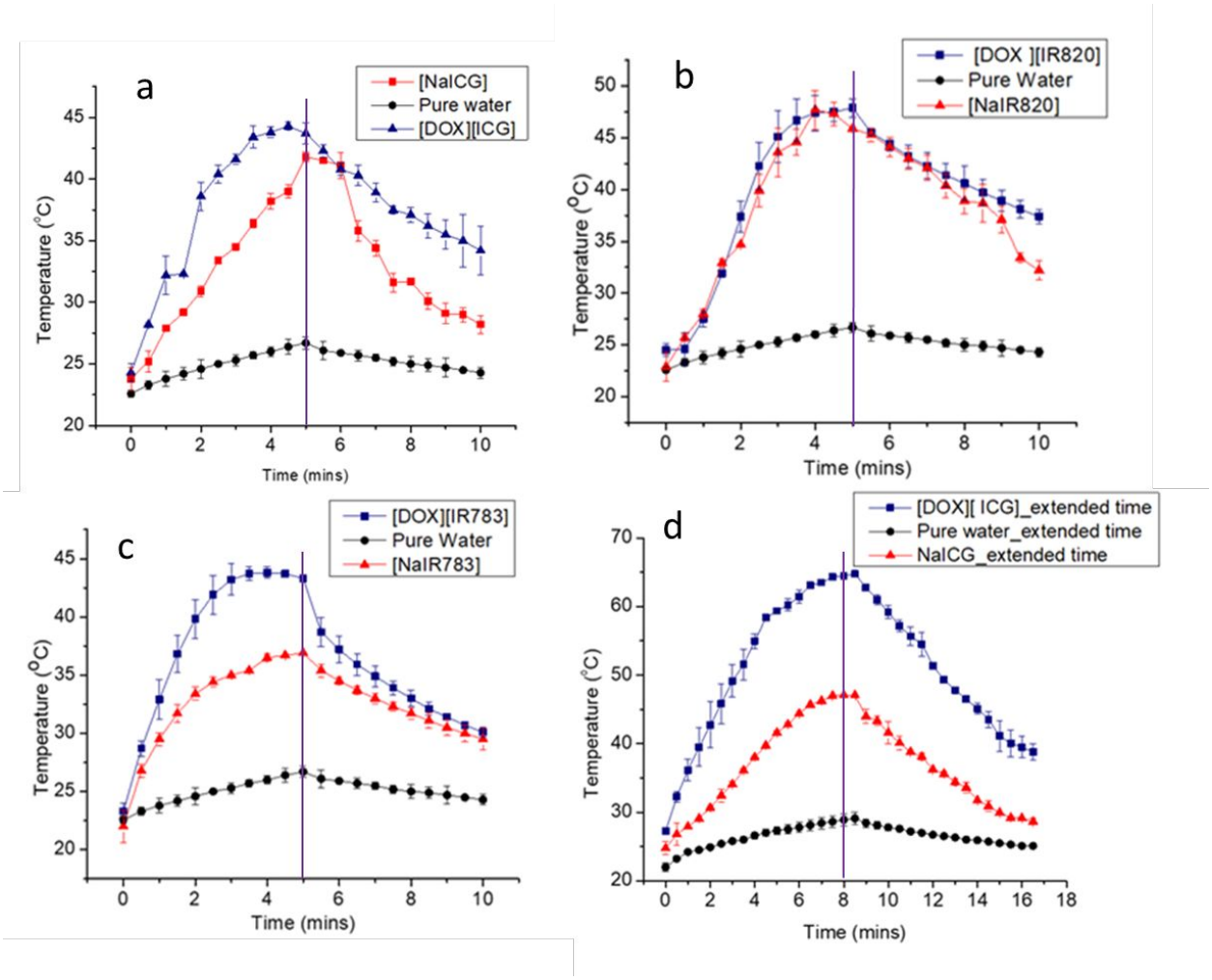

Figure S13. Light to heat conversion efficiency curve for a) [DOX][ICG] INMs and NaICG b) [DOX][IR820] INMs and NaIR820 c) [DOX][IR783] INMs and NaIR783 in pure water conducted for 5-10 mins. d) extended light to heat conversion efficiency curve for [DOX][ICG] and NaICG in water conducted for 8-16 mins. Error bars are presented as mean ± standard deviation (SD).

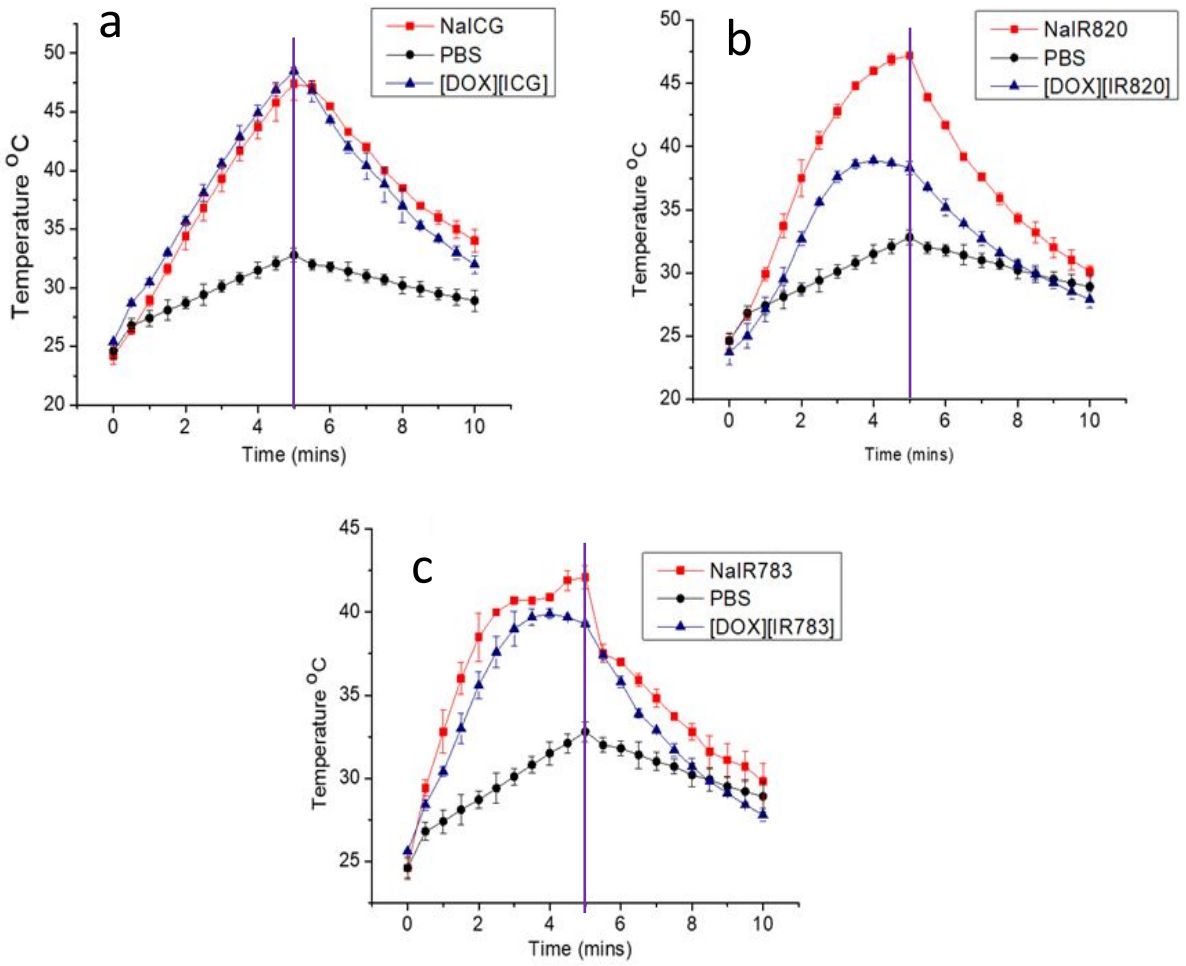

Figure S14. Light to heat conversion efficiency curve for a) [DOX][ICG] INMs and NaICG b) [DOX][IR820] INMs and NaIR820 c) [DOX][IR783] INMs and NaIR783 in PBS conducted for 5-10 mins. Error bars are presented as mean ± standard deviation (SD).

Photothermal Efficiency Equation.

Photothermal heat conversion efficiencies (**η**) of the INMs and parent drugs were determined using the following Equation S7-S10

$$\eta = \frac{hs(T_{max} - T_{surr}) - Q_{dis}}{I(1 - 10^{-A})} \text{ ----------(S7)}$$

Where h is the heat transfer coefficient, s represents the surface area of the container, and hs is obtained from Equation S10 and Figure S10. T_{max} is the steady state temperature of the INMs and for [DOX][IR783] it was found to be 44.5 ^{o}C (Figure S10c). The environmental temperature (T_{surr}) was 22.5 ^{o}C. The change in temperature (T_{max} - T_{surr}) for [DOX][IR783] INM was determined to be 22.0 ^{o}C. I indicate the laser power, which was 1 W for all samples. A represents absorbance of PTA. Q_{dis} is the heat dissipated from lights absorbed by solution and cuvette walls. Q_{dis} for INMs sample was determined from sample control with pure cell media and was found to be 17.2 mW. To determine hs, the following dimensionless parameter, **θ**, is introduced in Equation S8.

$$\theta = \frac{T - T_{surr}}{T_{max} - T_{surr}} \text{ ---------- } (S8)$$

Then, the time constant τs can be deduced from Equation S9.

$$t = -\tau s \, ln\boldsymbol{\theta} \text{--------} (S9)$$

Then, the time constant $\boldsymbol{\tau}_s$ of the [DOX][IR783] INMs sample was determined to be 287.5s. By inserting this value into Equation S10, hs can be calculated.

$$hs = \frac{m_D c}{\tau_s} \ldots\ldots\ldots (S10)$$

Where m_D is the mass of solution (1.0g) and C is the specific heat (4.2 J/g ^{o}C). hs for [DOX][IR783] was determined to be 14.6 mW/ ^{o}C. After substituting all parameters into Equation S4, **η** was determined to be 24.3 %

Table S9. Photothermal efficiency for all INMs and parent dyes in pure water and PBS

Compound	**η** % (pure water)	**η** % (PBS)
NaICG	34.72	17.06
[DOX][ICG] (INMs)	17.20	27.32
NaIR820	16.71	30.16
[DOX][IR820] (INMs)	13.23	12.84
NaIR783	8.23	15.08
[DOX][IR783] (INMs)	24.31	21.31

Singlet Oxygen Quantum yield

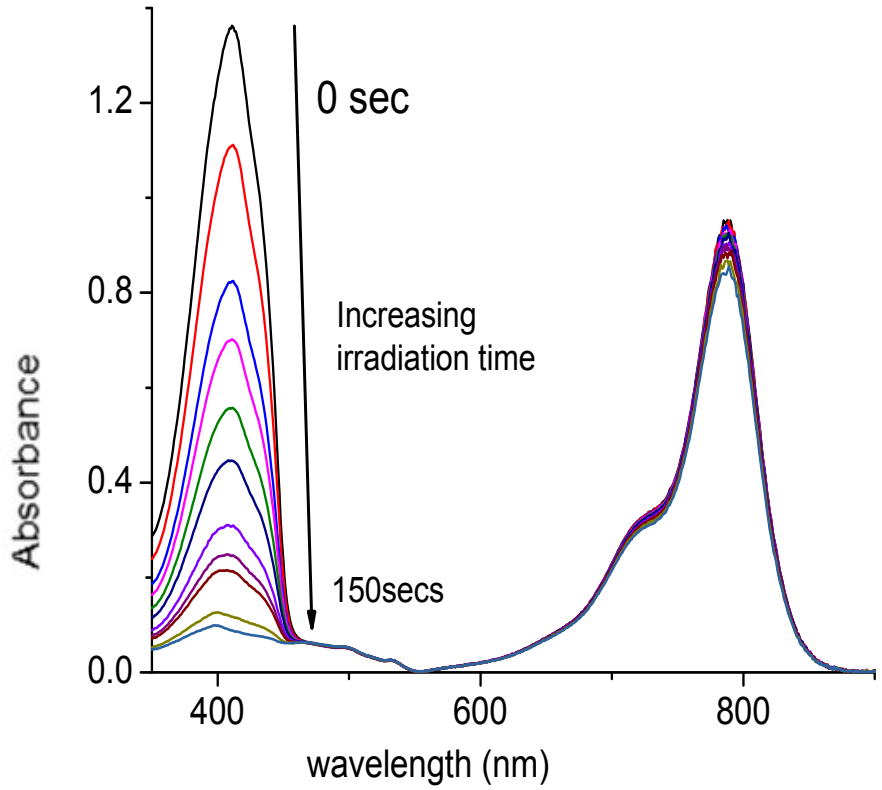

Figure S15. Photodegradation of DPBF upon increasing irradiation time in the presence of [DOX][ICG] in ethanol.

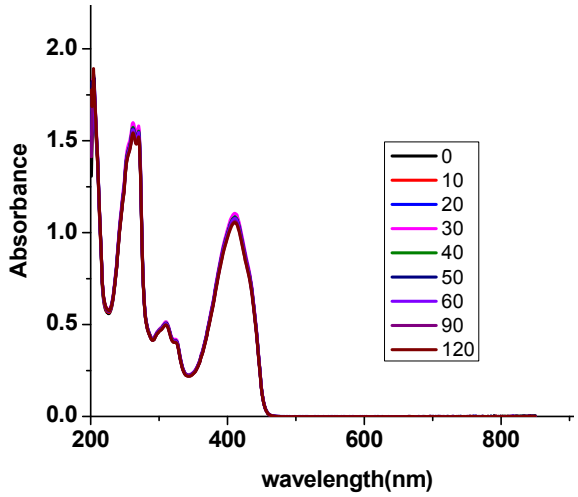

Figure S16. Absorbance of DPBF probe (411 nm) in ethanol after irradiation with 808 nm laser over increased time

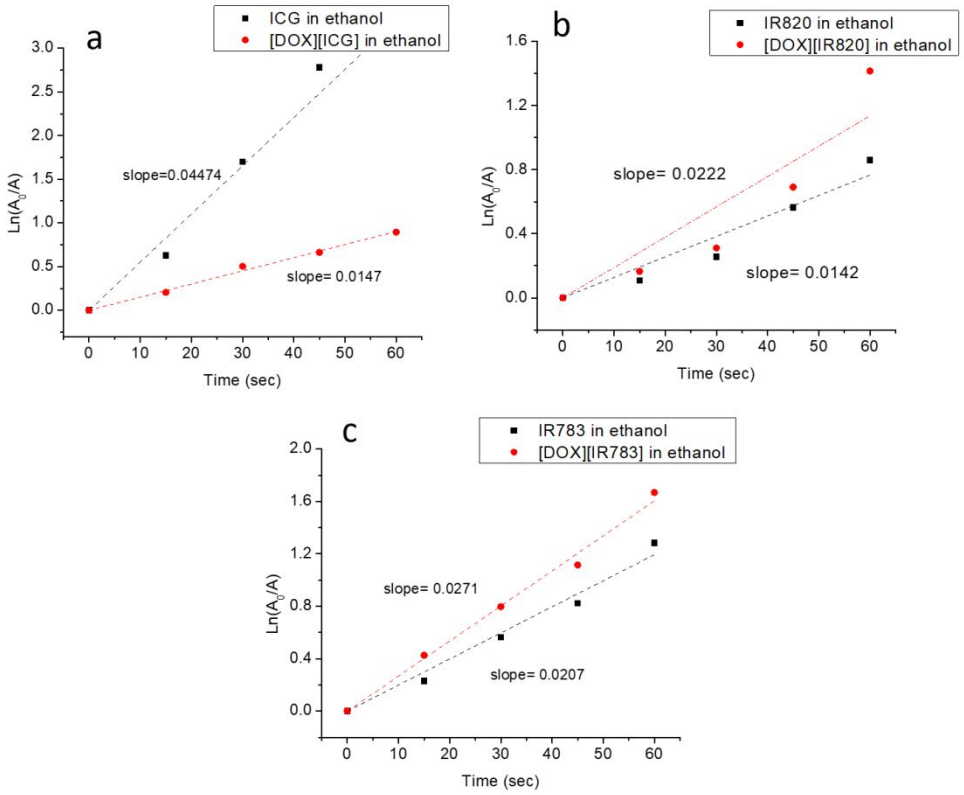

Figure S17. SOQY results in ethanol for a) NaICG and [DOX][ICG] b) NaIR820 and [DOX][IR820] c) NaIR783 and [DOX][IR783].

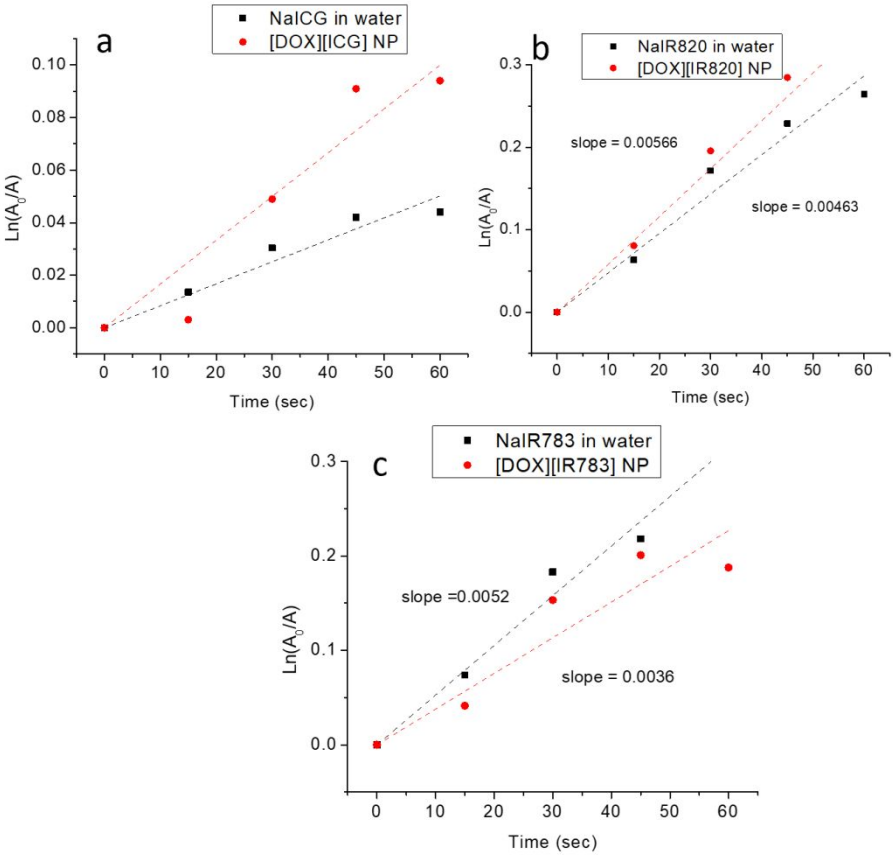

Figure S18. SOQY results in water for a) NaICG and [DOX][ICG] b) NaIR820 and [DOX][IR820] c) NaIR783 and [DOX][IR783]

Table S10. SOQY for the INMs and IMs respectively in water and ethanol respectively.

Drugs	Φ_Δ (INMs) %	Φ_Δ (IMs) %
NaICG	0.1	24.0
[DOX][ICG]	0.2	8.0
NaIR820	0.6	7.7
[DOX][IR820]	0.8	12.1
NaIR783	0.7	11.3
[DOX][IR783]	0.5	14.7

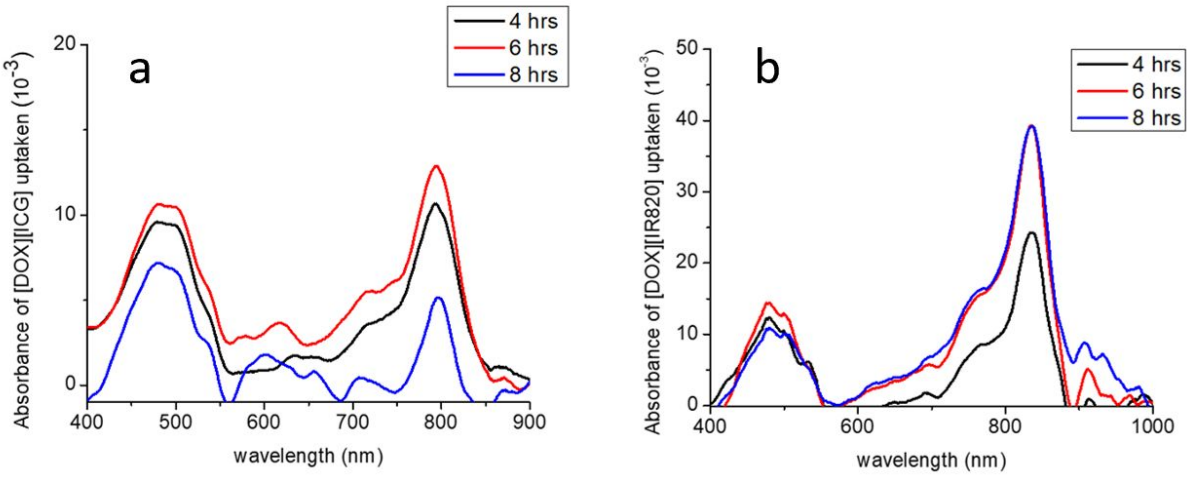

Figure S19. Time-dependent cellular uptake for a) [DOX][ICG] and b) [DOX][IR820] on MCF-7 cells.

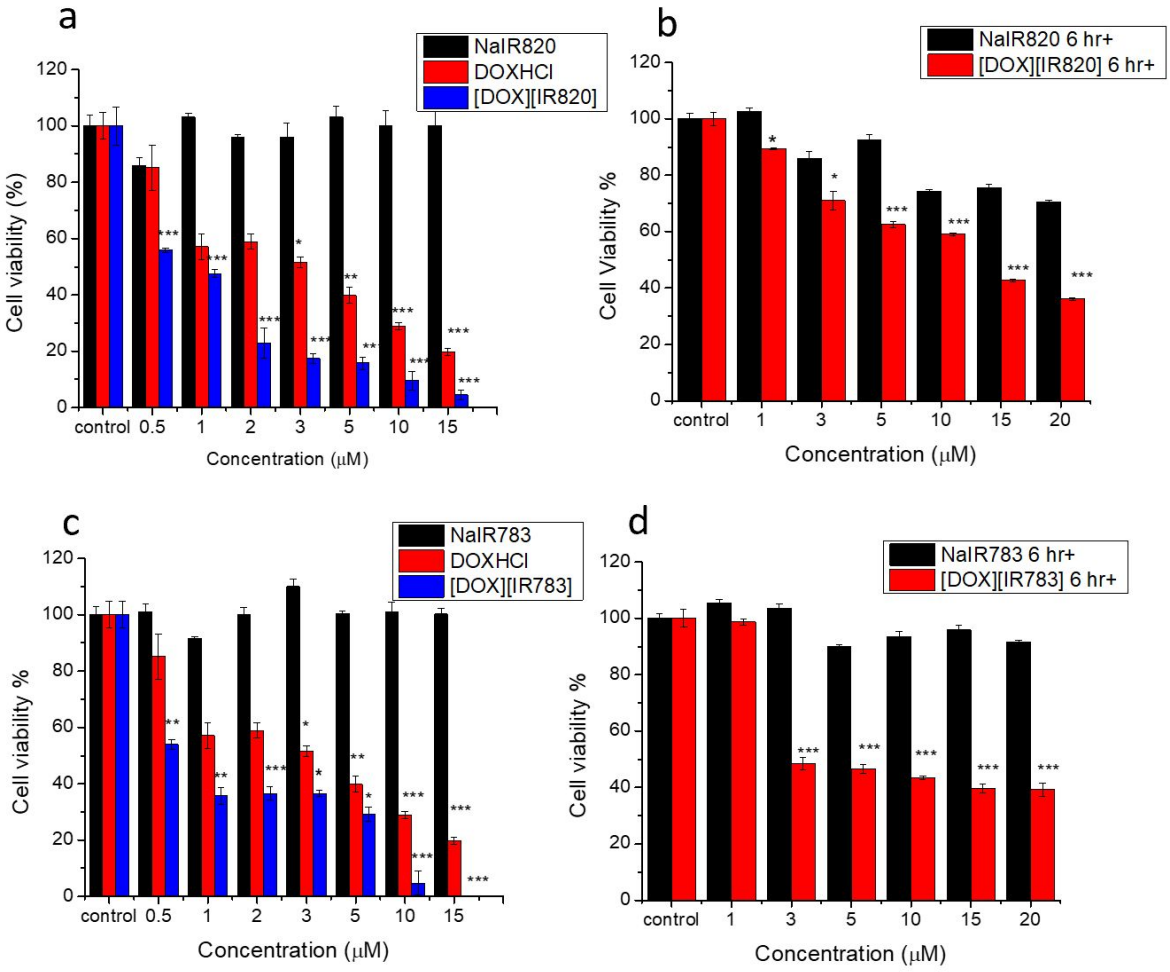

Figure S20. a) Cell viability results for varying concentrations of NaIR820 and doxorubicin-based drugs treated for 24 hr in the dark b) Cell viability results for NaIR820 and [DOX][IR820] INMs incubated for 6 hr and irradiated with 808 nm laser (1 Wcm^{-2}) for 5 min. c) Cell viability results for varying concentrations of NaIR783 and doxorubicin-based drugs treated for 24 hr in the dark d) Cell viability results for NaIR783 and [DOX][IR783] on MCF-7 breast cancer cell line treated for 6 hr and exposed to light. p values are determined using two-tailed student's t-test and are reported as *p< 0.05, **p< 0.01, ***p< 0.005.

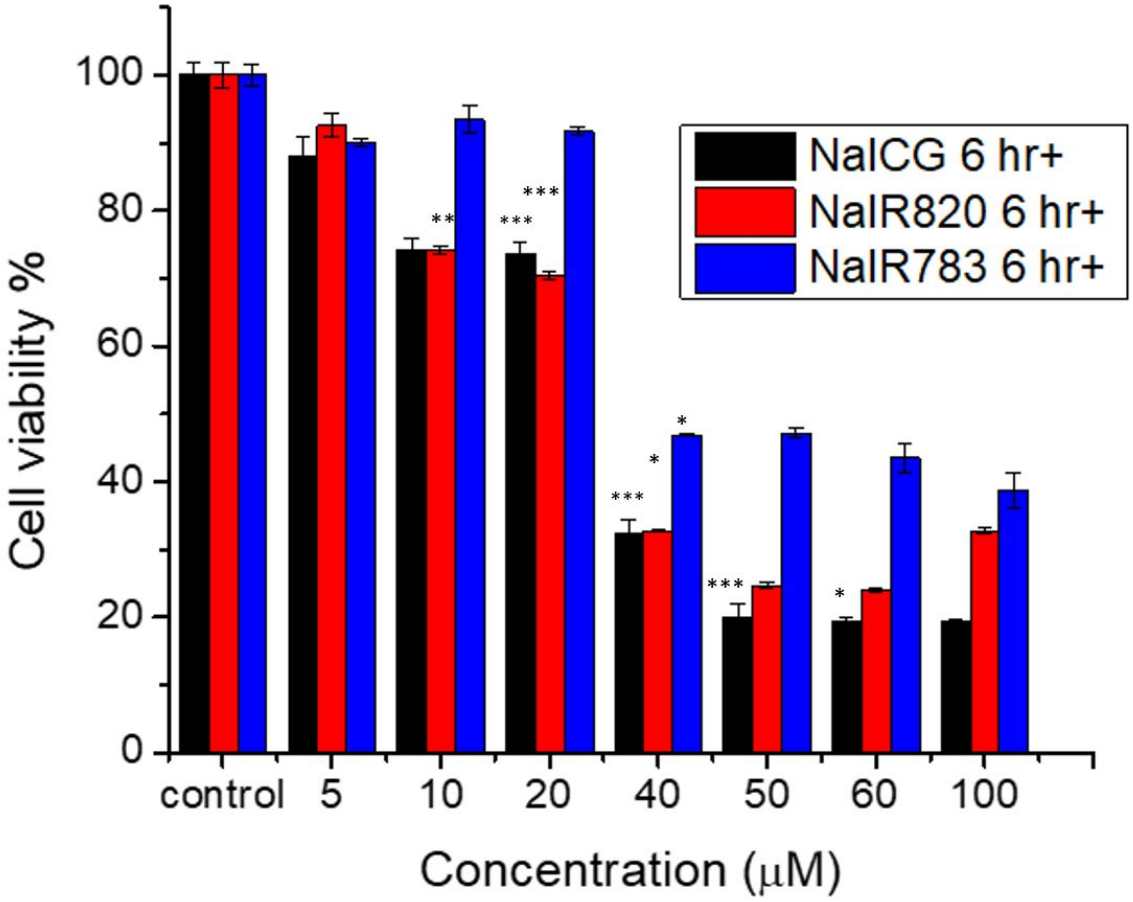

Figure S21. Cell viability results of parent PTT drugs on MCF-7 cell lines incubated for 6 hr and exposed to 1 Wcm^{-2} of 808 nm laser radiation for 5 min. p values are determined using two-tailed student's t-test and are reported as *p< 0.05, **p< 0.01, ***p< 0.005.

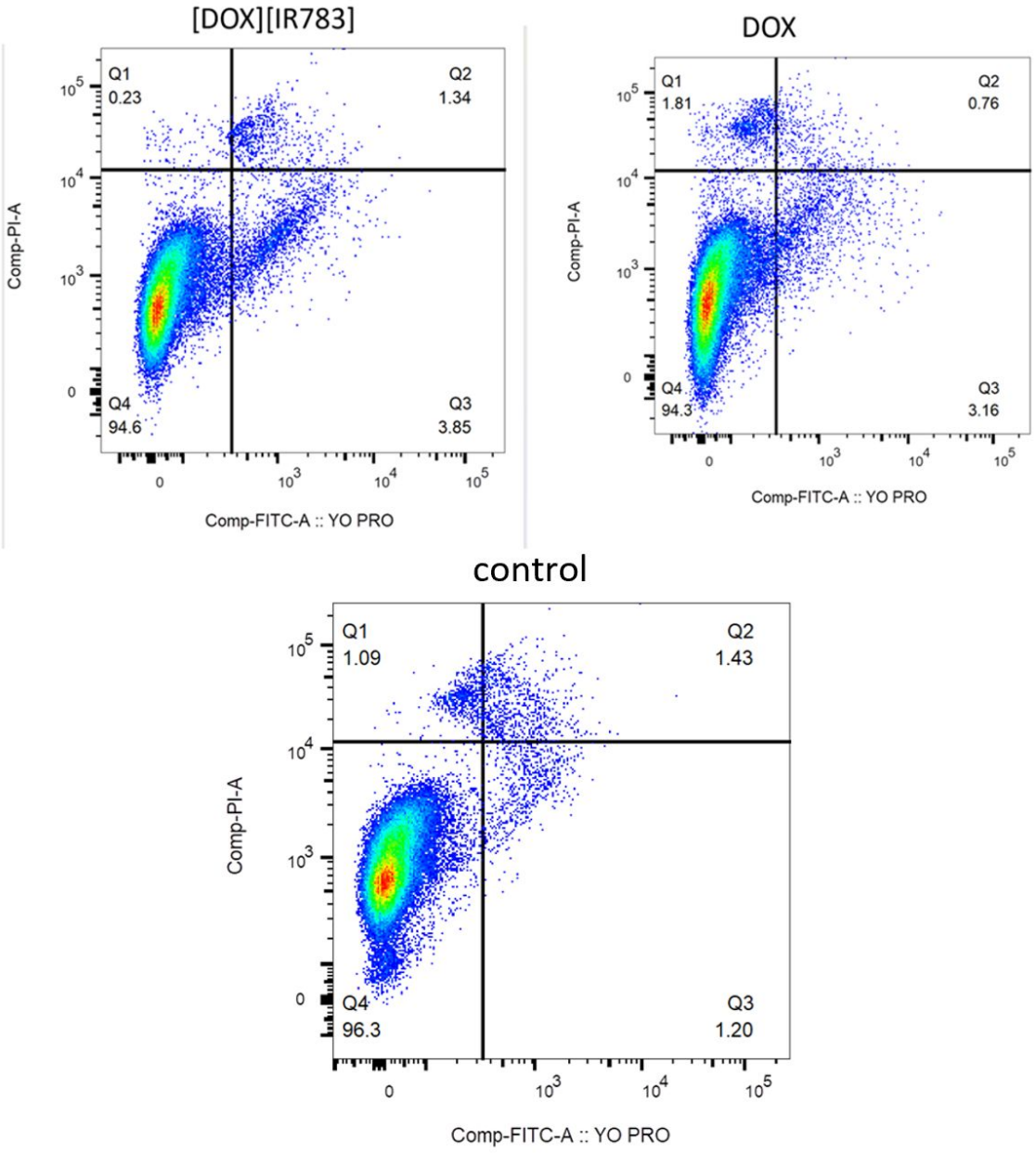

Figure S22. YO-PRO/propidium-iodide (PI) staining results for MCF-7 cells treated with [DOX][IR783] INMs and DOX after 6 hr drug incubation. Numbers in quadrants show percentages (%) of total cell populations.

Supplementary References

(1) Magde, D.; Wong, R.; Seybold, P. G. Fluorescence Quantum Yields and Their Relation to Lifetimes of Rhodamine 6G and Fluorescein in Nine Solvents: Improved Absolute Standards for Quantum Yields. *Photochem. Photobiol.* **2002**, *75* (4), 327.

(2) James, N. S.; Chen, Y.; Joshi, P.; Ohulchanskyy, T. Y.; Ethirajan, M.; Henary, M.; Strekowski, L.; Pandey, R. K. Evaluation of Polymethine Dyes as Potential Probes for near Infrared Fluorescence Imaging of Tumors: Part - 1. *Theranostics* **2013**, *3* (9), 692–702.

(3) Motlagh, N. S. H.; Parvin, P.; Ghasemi, F.; Atyabi, F. Fluorescence Properties of Several Chemotherapy Drugs: Doxorubicin, Paclitaxel and Bleomycin. *Biomed. Opt. Express* **2016**, *7* (6), 2400.